LOCAL MODELLING OF BACKFILL EFFECTS FOR RIGID AXISYMMETRIC FOUNDATIONS UNDER DYNAMIC EXCITATION

ZBIGNIEW SIENKIEWICZ

Koszalin University of Technology, Department of Civil and Environmental Engineering, Koszalin, Poland; e-mail: zbigniew.sienkiewicz@wbiis.tu.koszalin.pl

The influence of backfill on the dynamic response of rigid axisymmetric foundations is described as reaction of an independent layer. It leads to the solution of the kinematic interaction problem by means of the complex stiffness matrix of a supporting medium given by a specific increase in relation to the case of non-embedded foundations. The increases of stiffnesses are obtained in the closed-form from steady-state solutions to the equation of motion of an isotropic homogeneous medium under appropriate displacement boundary and radiation conditions. The approximate modelling is compared with results of the rigorous boundary integral equation approach.

Key words: kinematic interaction, embedded foundation, backfill, local modelling

1. Introduction

In the dynamic analysis of foundations supported on a soil, the foundation block is massive and may be considered as a rigid body. The excitation is assumed to be harmonic being able to consider other excitations by means of Fourier transform techniques. The steady-state motion of a massive foundation can be analysed in two steps. In the first step, also called "kinematic interaction", the response of a massless rigid body on a supporting medium is computed due to the dynamic excitation under consideration. The dynamic response is determined by the stiffness matrix of the supporting medium for a given shape of the foundation. It is worth to say that dynamic forces and displacements related by the stiffness matrix are generally out of phase. It is convenient then to use complex notation to represent forces and displacements of the foundation and stiffnesses of the supporting medium. The real

component of the stiffnesses reflects the stiffness and inertia of the soil. The imaginary component reflects the damping of the system. The main part of the damping is due to the energy dissipated by the waves propagating away from the foundation (radiation damping). In addition to the radiation damping, a hysteretic material damping may exist. Once the dynamic stiffness of the supporting medium is known, the response of the foundation including its mass may be evaluated from the general equations of translational and rotational motion of the massive rigid body.

Generally, the foundations are surrounded by a backfill, which modifies the dynamic stiffness of the supporting medium. The kinematic interaction problem is governed by a mixed boundary value problem of three-dimensional elastodynamics if the soil medium is treated as a continuum half-space. The procedures utilised to solve the problem include the finite element method, the boundary element method or hybrid approaches (Lysmer, 1980; Apsel and Luco, 1987; Mita and Luco, 1987; Emperador and Dominguez, 1987; Barros, 2006). Due to unbounded nature of the soil medium, the computational size of these methods is very large. Furthermore, the foundation embedment conditions are very complex practically due to uncertainties in the state of the soil. Then, approximate models are justified to supplement more generally applicable rigorous methods. Approximate approaches to model the embedment effects of rigid cylindrical foundations in the dynamic soil-structure interaction analysis include:

- a linear elastic weightless spring system (Prakash and Puri, 1988)
- an empirical approach (Gazetas, 1991)
- a lumped-parameter model (Wolf and Paronesso, 1992; Wu and Lee, 2002)
- a cone model (Meek and Wolf, 1994; Jaya and Prasad, 2002; Takewaki *et al.*, 2003; Wolf, 1994; Wolf and Preisig, 2003)
- an independent continuum layer (Novak *et al.*, 1977).

The objective of this paper is to present a dynamic local approach to model the backfill effects on complex stiffnesses of a supporting medium under following assumptions:

(1) the backfill is modelled as an independent isotropic homogeneous medium in the plane and (or) anti-plane strain cases;

(2) the medium is characterised by the mass density ρ_B and complex Lame's constants μ_B^*, λ_B^* to include material damping.

The backfill reduces the effect of embedment due to excavating and backfilling of the soil deposit in the place of building of the foundation. This fact can be taken into account by the appropriate choice of the mass density and dynamic material parameters. The parameters can be estimated by solution of the inverse problem if the dynamic response of the embedded foundation is given from measurements.

2. Statement of the problem

Let $\Omega = \Omega^I \cup \Omega^E \subset R^3$ be the domain in three-dimensional space R^3 occupied by a rigid massless inclusion Ω^I and an excavated elastic half-space Ω^E, see Fig. 1.
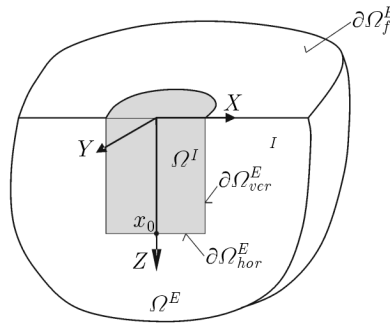
Fig. 1. Description of the model

The rigid massless body Ω^I is perfectly bonded to the half-space Ω^E along the surface $\partial \Omega_C^E = \partial \Omega_{hor}^E \cup \partial \Omega_{ver}^E$. The body $\Omega = \Omega^I \cup \Omega^E$ is in a state of motion relative to an inertial frame of reference.

2.1. Balance equations for the rigid massless inclusion Ω^I

The rigid massless inclusion Ω^I is subjected to the external force $\vec{P}_0(t) = \vec{P}_0 e^{i\omega t}$ and moment $\vec{M}_0(t) = \vec{M}_0 e^{i\omega t}$ vectors acting at the reference point $\boldsymbol{x}_0 \in \Omega^I$ with harmonic time dependence of the type $e^{i\omega t}$ in which ω is the circular frequency and $i = \sqrt{-1}$. Furthermore, due to deformation of the half-space Ω^E, it is loaded by a field $\vec{t}(\boldsymbol{x}, \boldsymbol{n}^I)$ of contact forces acting on $\partial \Omega^I$, where $\boldsymbol{n}^I$ is the unit outer normal vector for Ω^I at $\boldsymbol{x} \in \partial \Omega^I$.

The momentum balance equation and balance of angular momentum for the massless rigid inclusion Ω^I lead to

$$\vec{P}_0 e^{i\omega t} + \int_{\partial\Omega^I} \vec{t}(\boldsymbol{x}, \boldsymbol{n}^I) e^{i\omega t} \, dS = \vec{0} \qquad\qquad \boldsymbol{x} \in \partial\Omega^I$$

$$\vec{M}_0 e^{i\omega t} + \int_{\partial\Omega^I} (\boldsymbol{x} - \boldsymbol{x}_0) \times \vec{t}(\boldsymbol{x}, \boldsymbol{n}^I) e^{i\omega t} \, dS = \vec{0} \qquad \boldsymbol{x} \in \partial\Omega^I$$
(2.1)

2.2. Field equations for the excavated half-space Ω^E

The steady-state time-harmonic motion of the excavated half-space Ω^E includes the fields of displacement $\vec{u}(\boldsymbol{x}, t) = \vec{u}(\boldsymbol{x}) e^{i\omega t}$, strain $\overleftrightarrow{\varepsilon}(\boldsymbol{x}, t) = \overleftrightarrow{\varepsilon}(\boldsymbol{x}) e^{i\omega t}$ and stress $\overleftrightarrow{\sigma}(\boldsymbol{x}, t) = \overleftrightarrow{\sigma}(\boldsymbol{x}) e^{i\omega t}$, $\boldsymbol{x} \in \Omega^E$.

The principle of linear momentum with the conservation of mass on the assumption of small deformations leads to the Cauchy equation of motion in the frequency domain (Achenbach, 1973)

$$\nabla \cdot \overleftrightarrow{\sigma}(\boldsymbol{x}) + \rho \vec{b}(\boldsymbol{x}) = -\omega^2 \rho \vec{u}(\boldsymbol{x}) \qquad \boldsymbol{x} \in \Omega^E \qquad (2.2)$$

where $\vec{b}(\boldsymbol{x})$ stands for the body force vector, ρ is the mass density, ∇ denotes the del operator and $\nabla \cdot (\cdot)$ implies the divergence of $(\cdot)$.

The principle of the angular momentum provides the symmetry of stress tensor $\overleftrightarrow{\sigma}(\boldsymbol{x})$. The generalized Hooke's law in the frequency domain for a linear inelastic isotropic homogeneous medium is

$$\overleftrightarrow{\sigma}(\boldsymbol{x}) = \lambda^* \operatorname{tr} \overleftrightarrow{\varepsilon}(\boldsymbol{x}) \overleftrightarrow{1} + 2\mu^* \overleftrightarrow{\varepsilon}(\boldsymbol{x}) \qquad \boldsymbol{x} \in \Omega^E \qquad (2.3)$$

where $\operatorname{tr} \overleftrightarrow{\varepsilon}$ means the trace of $\overleftrightarrow{\varepsilon}$, $\overleftrightarrow{1}$ denotes the unit tensor and λ^* and μ^* are complex-valued Lame' constants.

The kinematical relation within the restrictions of the linearised theory is given by

$$\overleftrightarrow{\varepsilon}(\boldsymbol{x}) = \frac{1}{2}(\nabla \vec{u}(\boldsymbol{x}) + \vec{u}(\boldsymbol{x})\nabla) \qquad \boldsymbol{x} \in \Omega^E \qquad (2.4)$$

Substituting Eqs (2.3) and (2.4) into (2.2), leads to the Navier-Cauchy equation of motion

$$\mu^* \nabla^2 \vec{u}(\boldsymbol{x}) + (\lambda^* + \mu^*) \nabla\nabla \cdot \vec{u}(\boldsymbol{x}) + \rho \vec{b}(\boldsymbol{x}) = -\omega^2 \rho \vec{u}(\boldsymbol{x}) \qquad \boldsymbol{x} \in \Omega^E \quad (2.5)$$

where $\nabla^2 = \nabla \cdot \nabla$ is the Laplacian operator.

2.3. Elastodynamic problem for the excavated half-space in the frequency domain

The problem can be stated as follows: to find the solution to Navier-Cauchy equation of motion (2.5) with the boundary conditions

$$\vec{u}(\boldsymbol{x}) = \underline{\vec{u}}(\boldsymbol{x}) \qquad \boldsymbol{x} \in \partial\Omega_C^E$$

$$\vec{t}(\boldsymbol{x}, \boldsymbol{n}) = \boldsymbol{n} \cdot \vec{\sigma}(\boldsymbol{x}) = \mathrm{T}^{\boldsymbol{n}}(\vec{u}(\boldsymbol{x})) = \vec{0} \qquad \boldsymbol{x} \in \partial\Omega_f^E = \partial\Omega^E - \partial\Omega_C^E \tag{2.6}$$

where $\underline{\vec{u}}(\boldsymbol{x})$, $\boldsymbol{x} \in \partial\Omega_C^E$ is the prescribed displacement on $\partial\Omega_C^E$, $\boldsymbol{n}$ denotes the unit outward normal vector to $\partial\Omega^E$ and the operator $\mathrm{T}^{\boldsymbol{n}}$ is defined by

$$\mathrm{T}^{\boldsymbol{n}}(\cdot) = \lambda^* \boldsymbol{n}\nabla\cdot(\cdot) + 2\mu^* \boldsymbol{n}\cdot\nabla(\cdot)\overleftrightarrow{1} + \mu^* \boldsymbol{n}\times\nabla\times(\cdot) \tag{2.7}$$

The considered elastodynamic problem includes the boundary extended to infinity, then it is reasonable to require that the displacement at infinity must be bounded and that no wave can be reflected back from infinity. These conditions, called the radiation conditions are crucial in searching the unique solution in unbounded domains, particularly in time-harmonic problems (Eringen and Suhubi, 1975).

2.4. Coupling equations

The excavated half-space and the rigid inclusion substructures can be coupled by enforcing the compatibility and the equilibrium conditions at their common interface $\Omega^I \cap \Omega^E$. The response of the rigid massless inclusion Ω^I can be described by the displacement $\vec{U}_0(t) = \vec{U}_0 \mathrm{e}^{\mathrm{i}\omega t}$ and the small rotation $\vec{\Phi}_0(t) = \vec{\Phi}_0 \mathrm{e}^{\mathrm{i}\omega t}$ vectors at the point of reference $\boldsymbol{x}_0 \in \Omega^I$. Then, the compatibility of interaction displacements at the contact surface between the half-space and the inclusion requires that

$$\underline{\vec{u}}(\boldsymbol{x}) = \vec{U}_0 + \vec{\Phi}_0 \times (\boldsymbol{x} - \boldsymbol{x}_0) \qquad \boldsymbol{x} \in \Omega^I \cap \Omega^E \tag{2.8}$$

The equilibrium of interaction forces at the medium-inclusion interface requires that

$$\vec{t}(\boldsymbol{x}, \boldsymbol{n}^I) + \vec{t}(\boldsymbol{x}, \boldsymbol{n}) = \vec{0} \qquad \boldsymbol{x} \in \Omega^I \cap \Omega^E \tag{2.9}$$

and $\boldsymbol{n}^I = -\boldsymbol{n}$ on $\Omega^I \cap \Omega^E$.

Taking the equilibrium of interaction forces (2.9) in equations (2.1) into account and referring to an orthonormal basis $\{o; \hat{e}_1, \hat{e}_2, \hat{e}_3\}$ results in the matrix form

$$\{P_0\} = \int_{\partial\Omega_C^E} [g(\boldsymbol{x}; \boldsymbol{x}_0)]^\top \{\vec{t}(\boldsymbol{x}, \boldsymbol{n})\} \, dS \qquad \boldsymbol{x} \in \partial\Omega_C^E = \partial\Omega_{hor}^E \cup \partial\Omega_{ver}^E \tag{2.10}$$

where $\{P_0\} = (P_{01}, P_{02}, P_{03}, M_{01}, M_{02}, M_{03})^\top$, $\{\vec{t}\} = (t_1, t_2, t_3)^\top$, and

$$[g(\boldsymbol{x}; \boldsymbol{x}_0)] = \begin{bmatrix} 1 & 0 & 0 & 0 & (z - z_0) & -(y - y_0) \\ 0 & 1 & 0 & -(z - z_0) & 0 & (x - x_0) \\ 0 & 0 & 1 & (y - y_0) & -(x - x_0) & 0 \end{bmatrix} \qquad (2.11)$$

Since the tractions $\vec{t}(\boldsymbol{x}, \boldsymbol{n})$ on $\partial\Omega_C^E$ are linearly related to the displacement $\vec{U}_0$ and the rotation $\vec{\Phi}_0$ of the rigid inclusion Ω^I, the traction vector $\{\vec{t}(\boldsymbol{x}, \boldsymbol{n})\}$ can be written in the form

$$\{\vec{t}(\boldsymbol{x}, \boldsymbol{n})\} = [H^{\boldsymbol{n}}(\boldsymbol{x})]\{U_0\} \qquad (2.12)$$

where $\{U_0\} = (U_{01}, U_{02}, U_{03}, \Phi_{01}, \Phi_{02}, \Phi_{03})^\top$ and $[H^{\boldsymbol{n}}(\boldsymbol{x})]$ is the 3×6 matrix of contact tractions on $\partial\Omega_C^E$ for unit rigid-body displacements of the foundation corresponding to each of the six degrees of freedom. Substitution from (2.12) to (2.10) gives

$$\{P_0\} = [K(\boldsymbol{x}_0)]\{U_0\} \qquad (2.13)$$

in which

$$[K(\boldsymbol{x}_0)] = \int\limits_{\partial\Omega_C^E} [g(\boldsymbol{x}; \boldsymbol{x}_0)]^\top [H^{\boldsymbol{n}}(\boldsymbol{x})] \, dS \qquad \boldsymbol{x} \in \partial\Omega_C^E \qquad (2.14)$$

is the 6×6 dynamic stiffness matrix of the supporting medium, referred to the point of reference $\boldsymbol{x}_0$.

The K_{pq} component $(p, q = 1, 2, \ldots, 6)$ of the matrix is given by

$$K_{pq}(\boldsymbol{x}_0) = \int\limits_{\partial\Omega_C^E} \{g_p(\boldsymbol{x}; \boldsymbol{x}_0)\}^\top \{H_q^{\boldsymbol{n}}(\boldsymbol{x})\} \, dS \qquad \boldsymbol{x} \in \partial\Omega_C^E \qquad (2.15)$$

in which $\{g_p(\boldsymbol{x}; \boldsymbol{x}_0)\}$ corresponds to the p-th column of the matrix $[g(\boldsymbol{x}; \boldsymbol{x}_0)]$ and $\{H_q^{\boldsymbol{n}}(\boldsymbol{x})\}$ corresponds to the q-th column of the matrix $[H^{\boldsymbol{n}}(\boldsymbol{x})]$.

In the case of rigid foundations with a vertical axis of symmetry and $\boldsymbol{x}_0 = (0, 0, z_0)$ the integration can be done in cylindrical coordinates (r, θ, z) and the azimuthal dependence can be factored out. The displacement vector $\vec{u}(\boldsymbol{x}) = \vec{U}_0 + \vec{\Phi}_0 \times (\boldsymbol{x} - \boldsymbol{x}_0)$, $\boldsymbol{x} \in \Omega^I \cap \Omega^E$, on the medium-foundation interface can be written in the matrix form

$$\{u(\boldsymbol{x})\} = [g(\boldsymbol{x}; \boldsymbol{x}_0)]\{U_0\} \qquad (2.16)$$

where $\{u(\boldsymbol{x})\} = (u_r(\boldsymbol{x}), u_\theta(\boldsymbol{x}), u_z(\boldsymbol{x}))^\top$, $\{U_0\} = (U_{01}, U_{02}, U_{03}, \Phi_{01}, \Phi_{02}, \Phi_{03})^\top$ and the rigid body motion influence matrix is given by

$$[g(\boldsymbol{x}; \boldsymbol{x}_0)] = \begin{bmatrix} \cos\theta & \sin\theta & 0 & -(z-z_0)\sin\theta & (z-z_0)\cos\theta & 0 \\ -\sin\theta & \cos\theta & 0 & -(z-z_0)\cos\theta & -(z-z_0)\sin\theta & r \\ 0 & 0 & 1 & r\sin\theta & -r\cos\theta & 0 \end{bmatrix} \quad (2.17)$$

Considering the q-th component $(q = 1, 2, \ldots, 6)$ of the generalized displacement vector U_{0q} it is possible to write the corresponding displacement and traction components in the form

$$\{u_q(\boldsymbol{x})\} = \{g_q(\boldsymbol{x}; \boldsymbol{x}_0)\}U_{0q} = [A_q(\theta)]\{\overline{g}_q(r, z)\}U_{0q}$$
$$\{\vec{t}_q(\boldsymbol{x}, \boldsymbol{n})\} = \{H_q^n(\boldsymbol{x})\}U_{0q} = [A_q(\theta)]\{\overline{H}_q^n(r, z)\}U_{0q} \quad (2.18)$$
$$\boldsymbol{x} = (r, \theta, z) \in \Omega^I \cap \Omega^E \qquad q = 1, 2, \ldots, 6$$

The diagonal matrices $[A_q(\theta)]$ represent the azimuthal dependence of the q-th rigid-body motion and are given by

$$[A_1(\theta)] = [A_5(\theta)] = \operatorname{diag}(\cos\theta, \sin\theta, \cos\theta)$$
$$[A_2(\theta)] = [A_4(\theta)] = \operatorname{diag}(\sin\theta, -\cos\theta, \sin\theta) \quad (2.19)$$
$$[A_3(\theta)] = \operatorname{diag}(0, 0, 1) \qquad [A_6(\theta)] = \operatorname{diag}(0, -1, 0)$$

The vector $\{\overline{g}_q(r, z; z_0)\}$ corresponds to the q-th column of the matrix $[\overline{g}(r, z; z_0)]$

$$[\overline{g}(r, z; z_0)] = \begin{bmatrix} 1 & 1 & 0 & -(z-z_0) & (z-z_0) & 0 \\ -1 & -1 & 0 & (z-z_0) & -(z-z_0) & -r \\ 0 & 0 & 1 & r & -r & 0 \end{bmatrix} \quad (2.20)$$

Substitution of (2.18) into (2.15) and integration over θ from 0 to 2π leads to

$$K_{pq}(z_0) = 2\pi a_{pq} \int_{L_c} \{\overline{g}_p(r, z; z_0)\}^\top \{\overline{H}_q^n(r, z)\}r \, dL(r, z) \quad (2.21)$$

in which L_c represents the line defined by intersection of the rz-plane $(\theta = 0)$ and $\partial\Omega_C^E = \partial\Omega_{hor}^E \cup \partial\Omega_{ver}^E$ and the matrix

$$[a] = \frac{1}{2} \begin{bmatrix} 1 & 0 & 0 & 0 & 1 & 0 \\ 0 & 1 & 0 & 1 & 0 & 0 \\ 0 & 0 & 2 & 0 & 0 & 0 \\ 0 & 1 & 0 & 1 & 0 & 0 \\ 1 & 0 & 0 & 0 & 1 & 0 \\ 0 & 0 & 0 & 0 & 0 & 2 \end{bmatrix} \quad (2.22)$$

Equation (2.21) indicates that generalized force-displacement relationship
(2.13) for a rigid massless foundation bonded to the supporting medium sys-
tem can be written in the form

$$
\begin{Bmatrix} P_{01} \\ P_{02} \\ P_{03} \\ M_{01} \\ M_{02} \\ M_{03} \end{Bmatrix} = \begin{bmatrix} K_{HH} & 0 & 0 & 0 & K_{HM} & 0 \\ 0 & K_{HH} & 0 & -K_{HM} & 0 & 0 \\ 0 & 0 & K_{VV} & 0 & 0 & 0 \\ 0 & -K_{MH} & 0 & K_{MM} & 0 & 0 \\ K_{MH} & 0 & 0 & 0 & K_{MM} & 0 \\ 0 & 0 & 0 & 0 & 0 & K_{TT} \end{bmatrix} \begin{Bmatrix} U_{01} \\ U_{02} \\ U_{03} \\ \Phi_{01} \\ \Phi_{02} \\ \Phi_{03} \end{Bmatrix} \quad (2.23)
$$

where the terms K_{HH}, K_{MM}, $K_{HM} = K_{MH}$, K_{VV}, and K_{TT} are the horizon-
tal, rocking, coupling, vertical, and torsional stiffness functions, respectively.
The functions are referred to the point of reference $\boldsymbol{x}_0 = (0, 0, z_0)$ and can be
written in the form

$$
\begin{aligned}
K_{HH} &= GR(k_{HH} + \mathrm{i}a_0 c_{HH}) & K_{VV} &= GR(k_{VV} + \mathrm{i}a_0 c_{VV}) \\
K_{HM} &= GR^2(k_{HM} + \mathrm{i}a_0 c_{HM}) & K_{TT} &= GR^3(k_{TT} + \mathrm{i}a_0 c_{TT}) \quad (2.24) \\
K_{MM} &= GR^3(k_{MM} + \mathrm{i}a_0 c_{MM})
\end{aligned}
$$

in which G is a shear modulus of reference, R denotes the radius of cylindrical
foundation and $a_0 = \omega R / V_S$ is the dimensionless frequency defined on the
basis of the S-wave velocity of reference V_S. The terms k_{pq} and c_{pq} are the
normalized stiffness and damping coefficients, respectively.

The key step in the solution is the evaluation of the contact traction matrix
$[\overline{H}^n(r, z)]$, $(r, z) \in L_c = L_{hor} \cup L_{ver}$.

3. Local modelling

Within the region Ω^E one identifies a half-space subregion Ω^N to represent
the soil in its natural state and a layer Ω^B to represent the disturbed soil
(backfill): $\Omega^E = \Omega^N \cup \Omega^B$, see Fig. 2.

The perfect bonding exists only between the half-space Ω^N and the rigid
body Ω^I along the contact surface $\Omega^N \cap \Omega^I$ and between the layer Ω_B and
the body Ω^I along the contact surface $\Omega_B \cap \Omega^I$. It is assumed however that
at the horizontal interface $\Omega^N \cap \Omega^B$ between the half-space and the layer, the
condition of continuity of displacements is not satisfied and that the surfaces
$\partial\Omega^N$ and $\partial\Omega^B$ of the separated regions are free from tractions. Then, the
tractions at the base of the rigid body are equal to those of the body placed
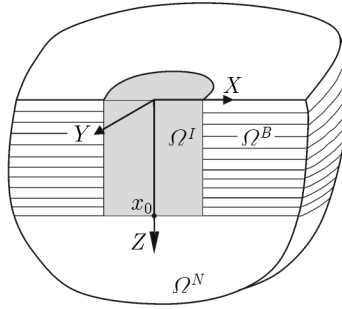
Fig. 2. Rigid body Ω^I on half-space Ω^N, surrounded by backfill layer Ω^B

on the soil surface, while the backfill reactions are to be evaluated independently by local modelling. These assumptions imply that the K_{pq} component $(p, q = 1, 2, \ldots, 6)$ of the dynamic stiffness matrix is given by

$$K_{pq}(z_0) = K_{pq}^0 + \Delta K_{pq}^B(z_0) \tag{3.1}$$

where K_{pq}^0 denotes the component for surface foundation and $\Delta K_{pq}^B(z_0)$ represents the increase due to local backfill reactions

$$\Delta K_{pq}^B(z_0) = 2\pi R a_{pq} \int_0^{H_B} \{\overline{g}_p(R, z; z_0)\}^\top \{\overline{H}_q^n(R, z)\} \, dz \tag{3.2}$$

where H_B is the thickness of the backfill layer.

The vector of contact tractions $\{\overline{H}_q^n\}$ can be obtained in a mathematically accurate form on the following assumptions:

(1) the backfill Ω^B is modelled as an inelastic isotropic homogeneous medium in the plane and (or) anti-plane strain cases

(2) the medium is characterised by complex Lame's constants μ_B^*, λ_B^* and mass density ρ_B.

The governing Navier-Cauchy equation of backfill motion as two-dimensional approximation of the three-dimensional case is derived directly from (2.5) and solved in cylindrical coordinates under appropriate displacement boundary conditions $\underline{\vec{u}}(\boldsymbol{x}) = \vec{U}_0 + \vec{\Phi}_0 \times (\boldsymbol{x} - \boldsymbol{x}_0)$, $\boldsymbol{x} \in \Omega^I \cap \Omega^B$ resulting from the rigid-body motion $\vec{U}_0$, $\vec{\Phi}_0$ of the inclusion Ω^I at the point of reference $\boldsymbol{x}_0 = (0, 0, z_0)$. The vectors of contact tractions $\{\overline{H}_q^n\}$ are given explicitly for all the six cases of unit rigid-body motions U_{0q}, $q = 1, \ldots, 6$

(1) $\{U_0\} = (1, 0, 0, 0, 0, 0)^\top$

$$\{\overline{H}_1^n\} = \left\{ \begin{matrix} (\lambda_B^* + 2\mu_B^*)\hat{s}_1^2 K_1(\hat{s}_1 R)A \\ -\mu_B^* \hat{s}^2 K_1(\hat{s}R)B \\ 0 \end{matrix} \right\} \tag{3.3}$$

where

$$\hat{s} = i\omega\sqrt{\frac{\rho_B}{\mu_B^*}} \qquad\qquad \hat{s}_1 = i\omega\sqrt{\frac{\rho_B}{\lambda_B^* + 2\mu_B^*}}$$

$$A = -\frac{L(\hat{s}, R)}{M(R)} \qquad\qquad B = -\frac{L(\hat{s}_1, R)}{M(R)}$$

$$L(s, R) = sK_0(sR) + 2R^{-1}K_1(sR)$$

$$M(R) = \hat{s}_1 \hat{s} K_0(\hat{s}_1 R)K_0(\hat{s}R) + \hat{s}_1 R^{-1}K_0(\hat{s}_1 R)K_1(\hat{s}R) +$$
$$+ \hat{s}R^{-1}K_1(\hat{s}_1 R)K_0(\hat{s}R)$$

and K_0, K_1 are the modified Bessel functions of the second kind,

(2) $\{U_0\} = (0, 1, 0, 0, 0, 0)^\top$

$$\{\overline{H}_2^n\} = \{\overline{H}_1^n\} \tag{3.4}$$

(3) $\{U_0\} = (0, 0, 1, 0, 0, 0)^\top$

$$\{\overline{H}_3^n\} = \left\{ \begin{matrix} 0 \\ 0 \\ -\mu_B^* \hat{s}\dfrac{K_1(\hat{s}R)}{K_0(\hat{s}R)} \end{matrix} \right\} \tag{3.5}$$

(4) $\{U_0\} = (0, 0, 0, 1, 0, 0)^\top$

$$\{\overline{H}_4^n\} = \left\{ \begin{matrix} (z_0 - z)\overline{H}_{12}^n \\ (z_0 - z)\overline{H}_{22}^n \\ -\mu_B^*\left[\dfrac{\hat{s}RK_0(\hat{s}R)}{K_1(\hat{s}R)} + 1\right] \end{matrix} \right\} \tag{3.6}$$

(5) $\{U_0\} = (0, 0, 0, 0, 1, 0)^\top$

$$\{\overline{H}_5^n\} = \left\{ \begin{matrix} -(z_0 - z)\overline{H}_{11}^n \\ -(z_0 - z)\overline{H}_{21}^n \\ \mu_B^*\left[\dfrac{\hat{s}RK_0(\hat{s}R)}{K_1(\hat{s}R)} + 1\right] \end{matrix} \right\} \tag{3.7}$$

(6) $\{U_0\} = (0,0,0,0,0,1)^\top$

$$\{\overline{H}_6^n\} = \left\{ \begin{array}{c} 0 \\ \mu_B^* \left[\dfrac{\hat{s}RK_0(\hat{s}R)}{K_1(\hat{s}R)} + 2 \right] \\ 0 \end{array} \right\} \tag{3.8}$$

The components ΔK_{pq}^B, $p,q = H, M, V, T$ of dynamic stiffness matrix of backfill (3.2) are found to be

$$\Delta K_{HH}^B = \pi \mu_B^* H_B \hat{a}_0^2 \frac{4K_1(\hat{a}_0)K_1(\hat{b}_0) + \hat{a}_0 K_0(\hat{a}_0)K_1(\hat{b}_0) + \hat{b}_0 K_1(\hat{a}_0)K_0(\hat{b}_0)}{\hat{a}_0\hat{b}_0 K_0(\hat{a}_0)K_0(\hat{b}_0) + \hat{a}_0 K_0(\hat{a}_0)K_1(\hat{b}_0) + \hat{b}_0 K_1(\hat{a}_0)K_0(\hat{b}_0)}$$

$$\Delta K_{HM}^B = \left(\frac{1}{2} H_B - z_0 \right) \Delta K_{HH}^B$$

$$\Delta K_{MM}^B = \left(\frac{1}{3} H_B^2 - H_B z_0 + z_0^2 \right) \Delta K_{11}^B + \pi \mu_B^* H_B R^2 \left[\frac{\hat{a}_0 K_0(\hat{a}_0)}{K_1(\hat{a}_0)} + 1 \right] \tag{3.9}$$

$$\Delta K_{VV}^B = 2\pi \mu_B^* H_B \hat{a}_0 \frac{K_1(\hat{a}_0)}{K_0(\hat{a}_0)}$$

$$\Delta K_{TT}^B = 2\pi \mu_B^* H_B R^2 \left[\frac{\hat{a}_0 K_0(\hat{a}_0)}{K_1(\hat{a}_0)} + 2 \right]$$

where

$$\hat{a}_0 = \mathrm{i}\omega R \sqrt{\frac{\rho_B}{\mu_B^*}} \qquad \hat{b}_0 = \hat{a}_0 \sqrt{\frac{\mu_B^*}{\lambda_B^* + 2\mu_B^*}} \tag{3.10}$$

4. Numerical results

Application of the closed-form solution require the model of material damping in the backfill to be specified. It is introduced by complex Lame's constants μ_B^* and λ_B^* of the form

$$\mu_B^* = \mu_B(1 + \mathrm{i}2\xi_S^B)$$
$$\lambda_B^* + 2\mu_B^* = (\lambda_B + 2\mu_B)(1 + \mathrm{i}2\xi_P^B) \tag{4.1}$$

where $\mu_B \equiv G_B$ and λ_B are real Lame's constants and ξ_S^B and ξ_P^B represent the hysteretic damping ratios for the S- and P-waves, respectively. The corresponding complex S- and P-wave velocities are

$$\hat{V}_S^B = V_S^B \sqrt{1 + \mathrm{i}2\xi_S^B} \approx V_S^B(1 + \mathrm{i}\xi_S^B)$$
$$\hat{V}_P^B = V_P^B \sqrt{1 + \mathrm{i}2\xi_P^B} \approx V_P^B(1 + \mathrm{i}\xi_P^B) \tag{4.2}$$

in which $V_S^B = \sqrt{\mu_B/\rho_B}$ and $V_P^B = \sqrt{(\lambda_B + 2\mu_B)/\rho_B}$ correspond to the real S- and P-waves velocities.

The complex Poisson ratio $\hat{\nu}_B$ is

$$\hat{\nu}_B = \frac{1 - 2\left(\frac{\hat{V}_S^B}{\hat{V}_P^B}\right)^2}{2\left[1 - \left(\frac{\hat{V}_S^B}{\hat{V}_P^B}\right)^2\right]} \approx \nu_B - \mathrm{i}(\xi_S^B - \xi_P^B)\frac{\left(\frac{V_S^B}{V_P^B}\right)^2}{1 - \left(\frac{V_S^B}{V_P^B}\right)^2} \tag{4.3}$$

where

$$\nu_B = \frac{1 - 2\left(\frac{V_S^B}{V_P^B}\right)^2}{2\left[1 - \left(\frac{V_S^B}{V_P^B}\right)^2\right]} \tag{4.4}$$

is real Poisson's ratio of the backfill.

The stiffness functions ΔK_{HH}^B, $\Delta K_{HM}^B = \Delta K_{MH}^B$, ΔK_{MM}^B, ΔK_{VV}^B and ΔK_{TT}^B expressed by Eqs. (3.9) and referred to the point of reference $\boldsymbol{x}_0 = (0, 0, H_B)$ can be written in the form analogous to (2.24)

$$\begin{aligned}
\Delta K_{HH}^B &= G_B R(k_{HH}^B + \mathrm{i}a_0^B c_{HH}^B) \\
\Delta K_{HM}^B &= G_B R^2(k_{HM}^B + \mathrm{i}a_0^B c_{HM}^B) \\
\Delta K_{MM}^B &= G_B R^3(k_{MM}^B + \mathrm{i}a_0^B c_{MM}^B) \\
\Delta K_{VV}^B &= G_B R(k_{VV}^B + \mathrm{i}a_0^B c_{VV}^B) \\
\Delta K_{TT}^B &= G_B R^3(k_{TT}^B + \mathrm{i}a_0^B c_{TT}^B)
\end{aligned} \tag{4.5}$$

in which $a_0^B = \omega R/V_S^B$ is the dimensionless frequency and the terms k_{mn}^B and c_{mn}^B denote the normalized stiffness and damping coefficients of the backfill, respectively. They depend on the dimensionless parameters:

$$k_{HH}^B, \ c_{HH}^B, \ k_{HM}^B = k_{MH}^B, \ c_{HM}^B = c_{MH}^B, \ k_{MM}^B, \ c_{MM}^B : \ H_B/R,$$
$$V_P^B/V_S^B, \ \xi_P^B, \ \xi_S^B, \ a_0^B; \ k_{VV}^B, \ c_{VV}^B, \ k_{TT}^B, \ c_{TT}^B : \ H_B/R, \ \xi_S^B, \ a_0^B \tag{4.6}$$

The normalized stiffness and damping coefficients have been calculated for the case of the backfill characterised by the values $H_B/R = 1$, $V_P^B/V_S^B \in \{\sqrt{2.25}, \sqrt{3}, \sqrt{3.94}, \sqrt{101}\}$, $\xi_P^B = 0.005$, $\xi_S^B = 0.01$ and a_0^B in the range from 0.25 to 6. To the given values of V_P^B/V_S^B there correspond the following values of Poisson's ratio $\nu_B \in \{0.1, 0.25, 033, 0.495\}$. Note that the range

Table 1

$a_0^B = \frac{\omega R}{V_S^B}$	$V_P^B/V_S^B = \sqrt{2.25}$ ($\nu_B = 0.1$)		$V_P^B/V_S^B = \sqrt{3}$ ($\nu_B = 0.25$)		$V_P^B/V_S^B = \sqrt{3.94}$ ($\nu_B = 0.33$)		$V_P^B/V_S^B = \sqrt{101}$ ($\nu_B = 0.495$)	
	k_{HH}^B	c_{HH}^B	k_{HH}^B	c_{HH}^B	k_{HH}^B	c_{HH}^B	k_{HH}^B	c_{HH}^B
0.25	3.010	11.234	3.244	12.078	3.438	12.843	4.228	17.308
0.50	3.399	9.429	3.642	10.138	3.833	10.791	4.302	14.666
0.75	3.587	8.803	3.814	9.480	3.973	10.110	3.755	13.778
1.00	3.691	8.505	3.890	9.179	4.000	9.816	2.744	13.394
1.25	3.754	8.340	3.924	9.025	3.979	9.682	1.326	13.233
1.50	3.797	8.239	3.942	8.938	3.945	9.620	−0.473	13.199
1.75	3.831	8.170	3.957	8.883	3.916	9.593	−2.638	13.250
2.00	3.858	8.121	3.974	8.846	3.899	9.580	−5.155	13.367
2.25	3.880	8.084	3.992	8.818	3.895	9.572	−8.014	13.538
2.50	3.899	8.054	4.011	8.794	3.901	9.565	−11.202	13.759
2.75	3.913	8.030	4.029	8.775	3.914	9.558	−14.706	14.025
3.00	3.924	8.010	4.046	8.758	3.931	9.550	−18.506	14.335
3.25	3.933	7.994	4.061	8.743	3.950	9.542	−22.582	14.687
3.50	3.938	7.979	4.074	8.729	3.970	9.533	−26.910	15.078
3.75	3.942	7.967	4.085	8.717	3.988	9.525	−31.459	15.508
4.00	3.943	7.957	4.093	8.707	4.004	9.516	−36.199	15.974
4.25	3.942	7.948	4.099	8.697	4.019	9.508	−41.095	16.473
4.50	3.940	7.940	4.103	8.689	4.032	9.500	−46.110	17.004
4.75	3.937	7.933	4.106	8.681	4.043	9.493	−51.204	17.561
5.00	3.933	7.927	4.106	8.674	4.051	9.486	−56.337	18.143
5.25	3.927	7.922	4.106	8.668	4.058	9.480	−61.472	18.744
5.50	3.921	7.917	4.104	8.662	4.063	9.474	−66.568	19.362
5.75	3.914	7.913	4.101	8.657	4.066	9.469	−71.589	19.990
6.00	3.906	7.909	4.096	8.653	4.068	9.464	−76.502	20.626

of Poisson's ratio cover fully drained ($\nu_B = 0.1$-0.2) to undrained ($\nu_B = 0.495$) conditions. The numerical results are presented in Tables 1, 2 and 3.

To validate the proposed approach, the impedance functions $K_{pq}(H_E)$, $p, q = H, M, V, T$ for the rigid massless cylindrical foundation embedded to a depth H_E in a uniform inelastic half-space are considered, where the point of reference is the centre of the bottom of the foundation ($z_0 = H_E$). The uniform half-space is characterised by complex-valued Lame's constants $\mu^* = \mu(1 + \mathrm{i}2\xi_S)$, $\lambda^* + 2\mu^* = (\lambda + 2\mu)(1 + \mathrm{i}2\xi_P)$, where $\mu \equiv G$ and λ are real Lame's constants and ξ_S and ξ_P represent the hysteretic damping ratios for the S- and P-waves, respectively. The corresponding complex S- and P-wave velocities are $\hat{V}_S = V_S(1 + \mathrm{i}\xi_S)$, $\hat{V}_P = V_P(1 + \mathrm{i}\xi_P)$, in which $V_S = \sqrt{\mu/\rho}$ and $V_P = \sqrt{(\lambda + 2\mu)/\rho}$ represent the real S- and P-waves velocities, respectively, and ρ is the mass density.

Table 2

$a_0^B = \frac{\omega R}{V_S^B}$	$V_P^B/V_S^B = \sqrt{2.25}$ ($\nu_B = 0.1$)		$V_P^B/V_S^B = \sqrt{3}$ ($\nu_B = 0.25$)		$V_P^B/V_S^B = \sqrt{3.94}$ ($\nu_B = 0.33$)		$V_P^B/V_S^B = \sqrt{101}$ ($\nu_B = 0.495$)	
	k_{MM}^B	c_{MM}^B	k_{MM}^B	c_{MM}^B	k_{MM}^B	c_{MM}^B	k_{MM}^B	c_{MM}^B
0.25	3.861	5.080	3.939	5.361	4.004	5.616	4.267	7.105
0.50	3.648	5.054	3.730	5.291	3.793	5.508	3.950	6.800
0.75	3.455	5.228	3.531	5.454	3.584	5.664	3.511	6.887
1.00	3.309	5.371	3.375	5.595	3.412	5.808	2.993	7.000
1.25	3.201	5.473	3.258	5.701	3.276	5.920	2.392	7.104
1.50	3.122	5.545	3.170	5.778	3.171	6.005	1.698	7.198
1.75	3.063	5.596	3.105	5.834	3.091	6.070	0.906	7.289
2.00	3.017	5.633	3.055	5.875	3.030	6.119	0.013	7.382
2.25	2.980	5.660	3.018	5.905	2.985	6.156	−0.984	7.478
2.50	2.951	5.680	2.988	5.927	2.951	6.184	−2.083	7.582
2.75	2.925	5.696	2.964	5.944	2.926	6.205	−3.281	7.694
3.00	2.903	5.707	2.944	5.956	2.906	6.220	−4.573	7.816
3.25	2.884	5.716	2.927	5.966	2.890	6.232	−5.955	7.947
3.50	2.866	5.724	2.911	5.973	2.876	6.241	−7.417	8.090
3.75	2.849	5.729	2.897	5.979	2.864	6.248	−8.951	8.243
4.00	2.833	5.734	2.883	5.984	2.853	6.254	−10.548	8.406
4.25	2.818	5.738	2.870	5.988	2.843	6.258	−12.195	8.580
4.50	2.803	5.741	2.857	5.990	2.834	6.261	−13.880	8.762
4.75	2.789	5.744	2.845	5.993	2.824	6.264	−15.591	8.953
5.00	2.775	5.746	2.833	5.995	2.814	6.266	−17.315	9.151
5.25	2.761	5.748	2.821	5.996	2.805	6.267	−19.039	9.355
5.50	2.748	5.749	2.808	5.998	2.795	6.268	−20.749	9.564
5.75	2.734	5.751	2.796	5.999	2.785	6.269	−22.434	9.777
6.00	2.721	5.752	2.784	6.000	2.775	6.270	−24.082	9.991

In accordance with the local modelling of embedment effects, the impedance functions K_{pq} are given by (3.1)

$$K_{pq}(H_E) \approx K_{pq}^0 + \Delta K_{pq}^B(H_E) \qquad (4.7)$$

where K_{pq}^0 denotes the component for surface foundation and $\Delta K_{pq}^B(H_E)$ represents the increase due to local backfill reactions at the point of reference $\boldsymbol{x}_0 = (0, 0, H_E)$. Assuming the parameters of backfill $\mu_B = \mu \equiv G$, $\lambda_B = \lambda$, $\rho_B = \rho$, $\xi_P^B = \xi_P$, $\xi_S^B = \xi_S$ and $H_B = H_E$, the functions $\Delta K_{pq}^B(H_E)$, $p, q = H, M, V, T$ can be calculated from equations (3.9) and (3.10) and expressed in form (4.5).

A test of all five impedance functions K_{HH}, $K_{HM} = K_{MH}$, K_{MM}, K_{VV}, and K_{TT} is realised by comparison of the results of Apsel and Luco (1987)

Table 3

$a_0^B = \frac{\omega R}{V_S^B}$	k_{VV}^B	c_{VV}^B	k_{TT}^B	c_{TT}^B
0.25	2.231	8.873	11.999	3.173
0.50	2.524	7.513	11.314	4.074
0.75	2.674	7.033	10.801	4.755
1.00	2.762	6.795	10.440	5.197
1.25	2.815	6.658	10.183	5.486
1.50	2.848	6.570	9.996	5.681
1.75	2.869	6.511	9.854	5.817
2.00	2.880	6.468	9.745	5.915
2.25	2.885	6.437	9.657	5.987
2.50	2.886	6.414	9.585	6.041
2.75	2.883	6.395	9.525	6.083
3.00	2.878	6.380	9.474	6.116
3.25	2.871	6.369	9.429	6.142
3.50	2.863	6.359	9.389	6.163
3.75	2.854	6.351	9.353	6.181
4.00	2.843	6.344	9.321	6.195
4.25	2.832	6.338	9.290	6.207
4.50	2.820	6.334	9.262	6.216
4.75	2.808	6.329	9.236	6.225
5.00	2.795	6.326	9.211	6.232
5.25	2.782	6.322	9.187	6.238
5.50	2.768	6.320	9.164	6.243
5.75	2.755	6.317	9.142	6.248
6.00	2.741	6.315	9.121	6.252

based on the rigorous non-singular integral equation approach to the dynamic response of embedded foundations with the values estimated from formula (4.7), where the functions K_{pq}^0 for the surface foundation were calculated by the approach of Wong and Luco (1976). The dimensionless normalized stiffness k_{pq} and damping c_{pq} coefficients defining the form of generalized force-displacement relationship given by (2.23) and (2.24) were calculated for embedment ratios $H_E/R = 0.25, 0.5, 1, 2$ at fixed values of $V_P/V_S = \sqrt{3}$, $\xi_P = 0.005$, $\xi_S = 0.01$. The calculations were performed for a number of values of the dimensionless frequency $a_0 = \omega R/V_S$ in the range from 0.25 to 6.00. Comparisons are presented in Figs. 3-7. Inspection of the Figures indicates that the stiffness coefficients for embedded foundations, obtained by the present approach, generally underestimate the values from the integral equation approach, with the exception of k_{VV} for $H_E/R = 1, 2$ where a small overestimation can be observed in limited ranges of the dimensionless frequency.

On the contrary, the damping coefficients determined by the present approach generally overestimate the values from the integral equation approach at low dimensionless frequencies and tend to the Apsel and Luco solution as frequency increases.
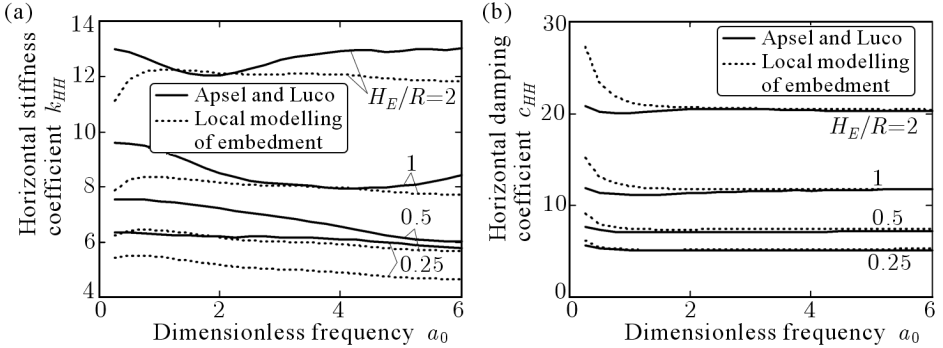
Fig. 3. Comparision of normalized horizontal stiffness and damping coefficients for cylindrical foundations with embedment ratios $H_E/R = 0.25$, 0.5, 1, 2: rigorous integral equation approach of Apsel and Luco (1987) – solid lines, local modelling of embedment – dotted lines
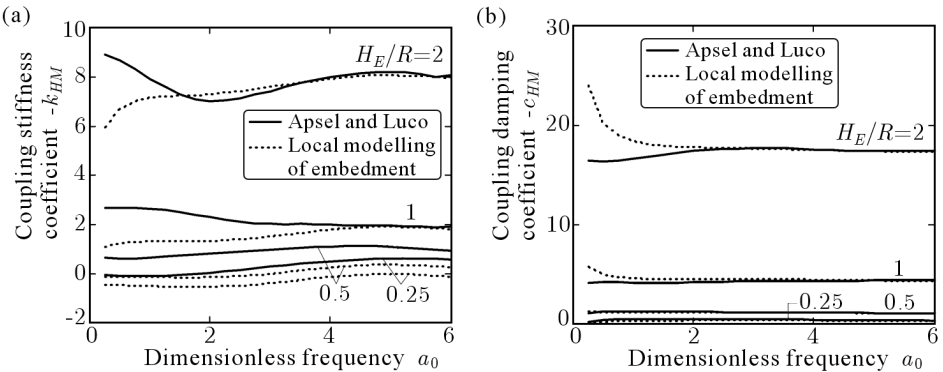
Fig. 4. Comparision of normalized coupling stiffness and damping coefficients for cylindrical foundations with embedment ratios $H_E/R = 0.25$, 0.5, 1, 2: rigorous integral equation approach of Apsel and Luco (1987) – solid lines, local modelling of embedment – dotted lines
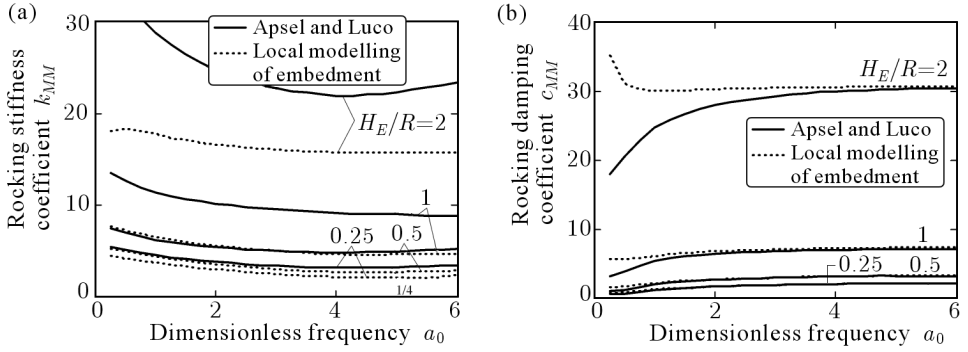
Fig. 5. Comparision of normalized rocking stiffness and damping coefficients for cylindrical foundations with embedment ratios $H_E/R = 0.25, 0.5, 1, 2$: rigorous integral equation approach of Apsel and Luco (1987) – solid lines, local modelling of embedment – dotted lines
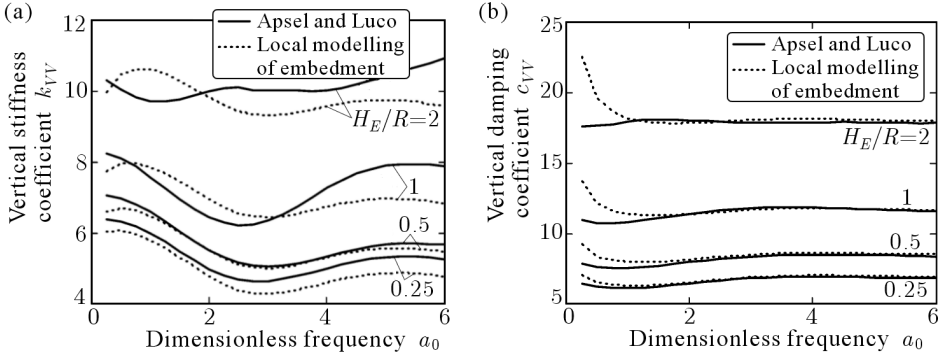
Fig. 6. Comparision of normalized vertical stiffness and damping coefficients for cylindrical foundations with embedment ratios $H_E/R = 0.25, 0.5, 1, 2$: rigorous integral equation approach of Apsel and Luco (1987) – solid lines, local modelling of embedment – dotted lines

5.   Conclusions

The dynamic generalized force-displacement relationship for a rigid massless foundation bonded to a supporting medium which represents the kinematic interaction can be expressed in the form of stiffness functions which depend on the soil properties, frequency of excitation and geometry of the foundation. On the assumption of local modelling of the backfill, the complex stiffnesses of the supporting medium are decomposed into the sum of two parts: the first one corresponding to the kinematic interaction of the rigid massless foundation placed on the surface of the supporting medium and the second one represen-
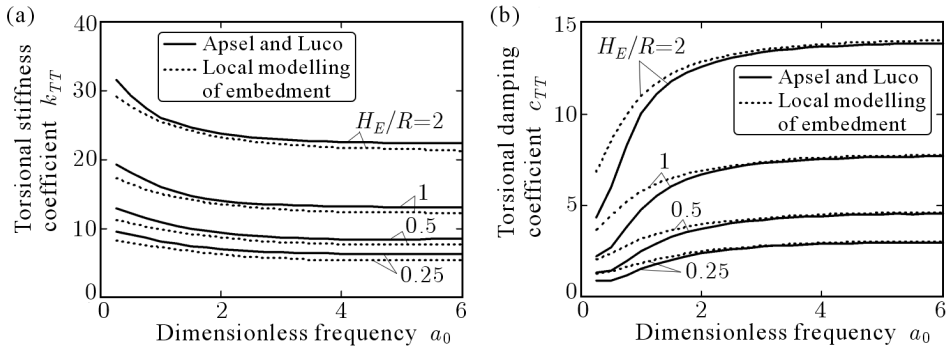
Fig. 7. Comparision of normalized torsional stiffness and damping coefficients for cylindrical foundations with embedment ratios $H_E/R = 0.25, 0.5, 1, 2$: rigorous integral equation approach of Apsel and Luco (1987) – solid lines, local modelling of embedment – dotted lines

ting the increases generated by the backfill. For rigid cylindrical foundations, the second part of the stiffness functions can be expressed in the closed-form. The accuracy of the simplified dynamic model is contained within the limits of the strength-of-materials approach to the foundation dynamics.

Once the response of a massless rigid foundation is computed, the dynamics of massive foundations can be studied by the methods of structural dynamics. Then, the presented local modelling is, among others, a simple, yet rational way to include the effect of backfill in the analysis of the dynamic response of embedded foundations, preferred in the preliminary stage of practical design.

References

1. ACHENBACH J.D., 1973, *Wave Propagation in Elastic Solids*, North-Holland, Amsterdam

2. APSEL R.J., LUCO J.E., 1987, Impedance functions for foundations embedded in a layered medium: an integral equation approach, *Earthquake Engineering and Structural Dynamics*, **15**, 213-231

3. BARROS P.L.A., 2006, Impedances of rigid cylindrical foundations embedded in transversely isotropic soils, *International Journal of Numerical and Analytical Methods in Geomechanics*, **30**, 683-702

4. EMPERADOR J.M., DOMINGUEZ J., 1987, Dynamic response of axisymmetric embedded foundations, *Earthquake Engineering and Structural Dynamics*, **18**, 1105-1117

5. Eringen A.C., Suhubi E.S., 1975, *Elastodynamics*, **2**, Academic Press, New York

6. Gazetas G., 1991, Formulas and charts for impedances of surface and embedded foundations, *Journal of Geotechnical Engineering (ASCE)*, **117**, 9, 1363-1381

7. Jaya K.P., Prasad A.M., 2002, Embedded foundation in layered soil under dynamic excitations, *Soil Dynamics and Earthquake Engineering*, **22**, 485-496

8. Lysmer J., 1980, Foundation vibrations with soil damping, *Civil Engineering and Nuclear Power, ASCE*, **II**, paper 10-4, 1-18

9. Meek J.W., Wolf J.P., 1994, Cone models for an embedded foundation, *Journal of Geotechnical Engineering (ASCE)*, **120**, 1, 60-80

10. Mita A., Luco J.E., 1987, Dynamic response of embedded foundations: a hybrid approach, *Computer Methods in Applied Mechanics and Engineering*, **63**, 233-259

11. Novak M., Nogami T., Aboul-Ella F., 1977, Dynamic soil reactions for plane strain case, *Journal of The Engineering Mechanics Division (ASCE)*, **104**, 953-959

12. Prakash S., Puri V.K., 1988, *Foundations for Machines: Analysis and Design*, Wiley, New York

13. Takewaki I., Takeda N., Uetani K., 2003, Fast practical evaluation of soil-structure interaction of embedded structures, *Soil Dynamics and Earthquake Engineering*, **23**, 195-202

14. Wolf J.P., 1994, *Foundation Vibration Analysis Using Simple Physical Models*, Englewood Cliffs, NJ, Prentice-Hall

15. Wolf J.P., Paronesso A., 1992, Lumped-parameter model for a rigid cylindrical foundations embedded in a soil layer on rigid rock, *Earthquake Engineering and Structural Dynamics*, **21**, 1021-38

16. Wolf J.P., Preisig M., 2003, Dynamic stiffness of foundation embedded in layered halfspace based on wave propagation in cones, *Earthquake Engineering and Structural Dynamics*, **32**, 1075-1098

17. Wong H.L., Luco J.E., 1976, Dynamic response of rigid foundations of arbitrary shape, *Earthquake Engineering and Structural Dynamics*, **4**, 579-587

18. Wu W.-H., Lee W.-H., 2002, Systematic lumped-parameter models for foundations based on polynomial-fraction approximation, *Earthquake Engineering and Structural Dynamics*, **31**, 1383-1412

Lokalne modelowanie wpływu zasypki na dynamicznie obciążane sztywne osiowo-symetryczne fundamenty

Streszczenie

Wpływ zasypki na dynamiczną odpowiedź sztywnych osiowo-symetrycznych fundamentów opisano jako reakcję niezależnej warstwy. Rozwiązanie problemu interakcji kinematycznej dane jest w postaci przyrostu zespolonej macierzy sztywności podłoża względem przypadku fundamentów niezagłębionych. Przyrosty sztywności otrzymano z rozwiązań w dziedzinie częstości równań ruchu izotropowego jednorodnego ośrodka z odpowiednimi przemieszczeniowymi warunkami brzegowymi i warunkami wypromieniowania. Modelowanie przybliżone porównano z wynikami numerycznego rozwiązania problemu w postaci brzegowego równania całkowego.